Stand-alone seawater RO (reverse osmosis) desalination powered by PV (photovoltaic) and PRO (pressure retarded osmosis)

He, W; Wang, Y; Shaheed, MH

Stand-alone Seawater Reverse Osmosis (RO) Desalination Powered by Photovoltaic (PV) and Pressure Retarded Osmosis (PRO)

Wei He, Yang Wang, and Mohammad Hasan Shaheed[1]

School of Engineering and Materials Science, Queen Mary, University of London, London E1 4NS, UK
E-mail: w.he@qmul.ac.uk, yang.wang@qmul.ac.uk, m.h.shaheed@qmul.ac.uk

Abstract:

A novel RO seawater desalination plant powered by PV and PRO (PVROPRO) is proposed and the feasibility of two stand-alone schemes, salinity-solar powered RO (SSRO) operation and salinity powered RO (SRO) operation, are investigated. First, the stand-alone feasibility of the plant is thermodynamically analysed. In doing so, on the basis of mathematical models describing RO, PRO and the PV array, the stand-alone feasibility is numerically investigated and the feasible operational windows for the two operation schemes, SSRO and SRO, are identified. In addition, the detrimental effects, concentration polarization (CP) and reverse salt permeation (RSP) in the mass transfer, on the operational windows are investigated. Finally, a case study of the proposed PVROPRO plant is developed based on the hourly solar data of Perth Australia in a year. The highest weekly production rate is found to be almost 20 times the rate in PVRO in the same week. Annual production is increased more than nine times compared to the stand-alone PVRO plant. Furthermore, it is found that, due to detrimental effects the weekly PW production rate is decreased in the range of 16-20% and the overall annual reduction is 18.07%.

Keywords: Stand-alone desalination plant, Hybrid salinity-solar power generation, Concentration polarization effect, Reverse salt permeation effect, optimal operation strategy

1. Introduction

Water is one of the most abundant resources on earth. However, most of it, about 97%, is saline water in the oceans and the remaining 3% is freshwater. The freshwater scarcity is becoming an increasingly significant problem in many areas around the world [1]. Desalination has been demonstrated to be a promising and viable technology to provide drinking water [2]. But the main issue impeding the wider use of desalination technologies is the high economic cost involved, especially due to intensive energy consumption [3]. In addition, current use of conventional fossil fuels as main power source is increasingly raising concerns over climate change and promoting global awareness for carbon dioxide emission reduction and cleaner energy supplies [4]. In fact, because of the shortage of freshwater, the opportunity for the use of renewable energy to power small seawater and brackish water desalination has become possible in many small cities and villages on the coastal areas and in many of the remote small villages and cities in the mainland [5]. Regions like Gulf Cooperation Council (GCC) countries [6] have many hours of sun shine which also makes solar energy an attractive source of renewable energy in those areas [7].

[1] Corresponding author: Tel: + 44 (0)20 7882 3774
E-mail address: m.h.shaheed@qmul.ac.uk

Actually, renewable energy powered reverse osmosis (RO) desalination and the optimum operation management have been widely studied in previous literatures [8-13]. Among the renewable energy powered RO desalination applications, stand-alone PVRO plant has been demonstrated to be feasible both in terms of techniques and costs in lab-scale and pilot-scale systems [14-17]. At present, it is considered as a proper solution for small-scale desalination applications in rural areas with high solar insulation [18]. The effectiveness of the stand-alone plant depends on the location, geographical conditions, topography of the site, and the capacity of the plant. Bilton et al. presented a generalised methodology to evaluate the feasibility of small-scale PVRO systems in challenging environment [19]. Their findings indicate that the freshwater cost of PVRO is economically feasible for most remote areas with high availability of solar energy [20]. Fraidenraich et al. proposed a simple and general theoretical procedure for estimating the specific energy consumption (SEC) to evaluate feasibility of a PVRO plant and validate the methodology with experiments [21]. During the last decade, with the significant development in optimal designs [22, 23] and control strategies [24, 25] for PVRO plants, the cost of freshwater has considerably reduced. However, the sunshine is not available at night. In order to prolong the operational hours, and to increase the renewable energy supply, alternative power sources need to be identified and integrated to the designs for night time operation. Previous investigations have focused on a hybrid system combining solar and wind energy to power RO desalination processes [26, 27]. An estimation of energy and water production during a large-scale time frame from photovoltaic-wind hybrid system coupled with RO desalination unit was developed based on the local solar and wind data [28]. Their results demonstrated the appropriation of the proposed hybrid system to produce water from brackish water (6 g/L) in southern Tunisia. Novosel et al. evaluated the impact of desalination in combination with water pump storage and penetration of wind and solar energy [29]. The analysis of the case study in Jordan demonstrated that the integration of water and renewable energy generation could provide a real benefit to the country water supply, energy security and ecology [29]. Recently, osmotic energy from water with different salinities has emerged as a viable alternative. Compared with other renewable energy sources, osmotic energy is less periodic and has no significant operational hazards. It therefore has the potential to formulate a hybrid energy system to supplement the power supply.

Pressure retarded osmosis (PRO) is one of the most investigated technologies in osmotic energy harvesting [30]. In a PRO plant, because of the osmotic pressure difference across the membrane, fresh water permeates from the unpressurized feed solution to the pressurised draw solution. Then, the pressurised permeation is expanded in a hydro-turbine to generate electricity [31]. Following the rapid developments made in the area of high performance membrane in the last decade, it has started to be utilised in reality [32]. In 2009, the world's first PRO salinity power plant was launched in Norway with a 4kW capacity [33]. In prior studies, PRO process has been investigated not only as an independent power plant [34-36], but also as an osmotic energy recovery device (ERD) positioned in pre- or post-treatment in hybrid RO-PRO plant frameworks [37, 38]. Compared with other current ERDs for RO desalination plants (e.g. pressure exchangers and hydro turbines), the second law efficiency of the PRO is relatively high [39]. Feinberg et al. carried out a theoretical study on a hybrid RO desalination plant with two-stage PRO osmotic ERD and indicated significant recoverable energy from mixing concentrated and dilute waters. [40]. Sharqawy and Banchik derived systematic effectiveness-mass transfer units (ε-MTU) models of the RO and PRO plants which are significantly helpful for engineers in the design [41, 42]. Also, an experimental pilot system was designed and constructed to investigate the reduced RO energy consumption by integrating with PRO [43, 44]. The

experiments showed that the enhanced power densities for the RO-PRO system ranged from 1.1 to 2.3 W/m^2 and indicated that future RO-PRO systems may reduce the specific energy consumption requirements for desalination by ~1 kWh/m^3 [44]. A thermodynamic analysis on a stand-alone salinity power driven RO plant is developed and, for the first time, the feasible conditions of the stand-alone salinity power supply is identified in a desalination application [45]. However, as suggested in the literature, no research has addressed the potential integration of the salinity energy with other renewable energy sources. Thus, this study aims to investigate the integration of salinity power and solar power and to identify the optimum operations of this hybrid renewable system in a desalination application.

Furthermore, the detrimental effects, including internal concentration polarization (ICP), external concentration polarization (ECP) and reverse solute permeation (RSP), are inevitable in a real PRO plant. These detrimental effects significantly reduce the performance of PRO salinity power generation. Banchik et al. investigated the overall membrane performance and the optimum operations of PRO plant based on ε-MTU model by evaluating the effect of CP, and found a reduction in performance [46]. Zwan et al. derived a hydrodynamic mass transfer model for a PRO process which accounted for the actual size of the membrane sheet and concluded that it is feasible to produce 0.5 MW with 1 m^3/s of freshwater [47]. Kim et al. modified the PRO models in order to incorporate the spatial distribution of concentration and the velocity in the two flow channels, and compared four different RO-PRO hybrid configurations [48]. Recently, Feinberg et al. demonstrated that the power densities achievable from PRO are well below those predicted by extrapolating lab-scale measurement with an idealised model and stated that future work should focus on increasing salinity difference and identifying optimum operating conditions [49]. Thus, using brine from RO is a natural solution to increase the initial salinity concentration difference. However, so far no research has addressed ICP, ECP and RSP effects on salinity energy generation in a hybrid RO-PRO plant. Therefore, further investigation is needed to address these issues.

Although several previous studies have focused on the salinity energy powered RO desalination plant, it is still a challenge to develop the stand-alone salinity power driven desalination based on the current PRO membrane performance. In fact, to deal with the problems in a stand-alone renewable energy powered system, a hybrid renewable energy source is a promising solution [50-52]. There are a large number of examples of stand-alone renewable energy powered systems at off-grid locations. An experimental study of hybrid energy generation including PV, wind emulator, battery, and controller was constructed and demonstrated to be capable to operate stand-alone mode and grid-connected mode [53]. A work of the solar PV and the solar/hydro schemes for rural electrification was evaluated and shown to be more reliable and sustainable than the use of a diesel genset [54]. A similar application for off-grid rural electrification by hybrid diesel power plant with high-penetration renewable and compressed air energy storage was also found in literatures [55]. Moreover, optimum design and control of the integrated PV and wind powered RO desalination plant was illustrated by a series of simulations to demonstrate applicability and effectiveness [56, 57]. Therefore this study focuses on investigating the hybrid solar-salinity energy supply in a RO desalination application to improve the freshwater production. In fact, the hybrid solar-salinity power generation has several advantages: i) the salinity power improves the energy efficiency of the solar powered system by the recovery of osmotic energy during daytime and by prolonging the operational hours over night through salinity power harvest; ii) the solar power helps improve the total water production of the hybrid RO-PRO system by providing external power to compensate the lack of commercially high performance PRO membrane in osmotic energy extraction currently in practice. Therefore, in the

hybrid system, the stand-alone feasibility can be realised by two operations: hybrid power source of salinity power from PRO and solar power from PV array during daytime, and only salinity power at night. With the osmotic energy generation, more freshwater can be treated under the available solar radiation. Conversely, at lower RO water recovery, salinity power generated by PRO is potentially capable to sustain continuous operation when the sun is unavailable. Such integration of power supplies ensures that the desalination plant meets the demand for the freshwater production. To this end, a study on the stand-alone RO desalination plant powered by PV and PRO is developed. First, the hybrid plant is proposed and thermodynamically analysed using a state-diagram. Following this, the stand-alone feasibility of the plant is studied and derived mathematically. Based on the models, the performance of the RO plant and the entire hybrid system is evaluated. The feasible operational windows of the two operations are identified and discussed. Finally, with the known hourly solar data available for Perth, Australia, over duration of a year, a case study of the proposed hybrid powered RO desalination is presented.

2. Stand-alone seawater RO desalination plant powered by hybrid system of PV and PRO

A proposed stand-alone solar-salinity power driven RO desalination system is illustrated in Fig. 1 and it shows the three main sub-systems in this hybrid plant. The hybrid system consists of RO desalination and renewable power generation including solar and salinity power; the two parts are closely interacted. The renewable energy generation supplies the power to the desalination plant and the brine from the RO desalination is the source of the chemical potential for salinity power generation. In operations of solar-salinity powered RO (SSRO) during daytime, both the PV array and the PRO plant are working to generate electricity. In contrast, at night in operations of salinity powered RO (SRO), only the PRO plant is working. In Fig. 1(b), the detail diagram of the hybrid plant is plotted. Seawater (SW) is pressurised by a high-pressure pump (HP) and a hydraulic ERD before it flows into a RO membrane module. The implementation of ERD can significantly reduce the exergy destruction of the RO plant [12]. The HP is driven by the induction motor. The freshwater is produced from the SW in the RO plant. Accordingly, two streams flow out from the RO module: the product water (PW) and the concentrated brine water (CW). The CW is further used to pressurise the SW in the ERD before it flows into the PRO plant, and the PW is the product of the hybrid system. In another sub-system, the solar power is harvested by solar PV technology and the salinity power is generated by the PRO plant. The low concentration streams (secondary wastewater and BW or their mixture) are the potential candidates for the feed solution of the osmotic membrane process [58]. In this study, impaired water (IW) is selected as the feed solution for the early-stage investigation. In order to overcome the pressure loss along the flow channel, the IW is pressurised by a boost pump (BP) which is also driven by the induction motor. Finally, the draw solution including the permeated water from the PRO feed solution is expanded in a hydro-turbine (HT) to generate electricity. Both renewable energy generators, the PV array and the PRO plant, are interconnected to an AC bus through DC/DC/AC and AC/DC/AC converters. For simplicity, the efficiencies of all the converters and motors are assumed to be 100%.

2.1. Thermodynamic analysis of the stand-alone salinity-solar power driven seawater RO plant

Before further analysis of the hybrid system, some key states of the saline streams are presented in the pressure-flow rate (P-Q) diagram as illustrated in Fig. 2. As can be seen from the diagram, the

pressure loss in the membrane and flow channels is negligible compared with the hydraulic pressure applied on the saline streams. So the applied pressure is considered as constant. Also, it is assumed that no fouling or membrane deformation is occurred. And because a very small amount of energy is used by the BP compared to the energy consumed by the HP, in this study, the energy consumption is only considered as the work of the HP in the RO sub-system.

In the P-Q diagram, the energy consumption by the RO plant and the energy generation by the PRO plant can be represented by the areas illustrated in Fig.2, i.e., the energy consumed can be represented by the area O-0-1-C, the energy recovered by ERD can be represented by the area 3-2-C-B and the energy generated by the PRO plant can be represented by the area O-5-4-B. These areas are determined by the specific states of the saline streams, namely states 2, 4 and 5 in Fig. 2. Moreover, these states of the saline streams can be controlled by the operations of the RO and PRO plants. Other states are usually determined by the local conditions or/and RO thermodynamic restrictions (TR) [59]. Therefore, this 'salinity cycle' has similar attributes as the classical thermodynamic cycles by changing states of the salinity concentration [45].

Two operational strategies in this hybrid power system are hybrid power of salinity and solar and stand-alone salinity power, namely SSRO and SRO operation. In the SRO operation, without the solar energy harvesting, the overall energy surplus between the generation and consumption by the hybrid system can be represented as the difference between the areas D-1-2-3 and 0-5-4-D. In contrast, in SSRO operation, the overall energy surplus includes the electricity generated from the PV array. Therefore, the overall energy surplus can be represented as

$$\begin{aligned} \Delta E^{SSRO} &= E_{PV} + E_{PRO} - W_{RO} \\ \Delta E^{SRO} &= E_{PRO} - W_{RO} \end{aligned} \tag{1}$$

where E_{PV}, E_{PRO} and W_{RO} are the energy generated from the PV array, energy generated from the PRO plant and the energy consumed by the RO-ERD plant, respectively. If the overall energy surplus is non-negative, theoretically, the hybrid system can be operated as stand-alone. Otherwise, the hybrid system needs an extra power source to cover the exceeding energy consumption. Therefore in the hybrid system, the stand-alone feasibility is determined by the states of the streams and the availability of the solar irradiation. In the SSRO operation, due to the availability of the solar PV power, more freshwater can be separated from the saline stream as illustrated in Fig. 2(a). Thus, it allows higher applied hydraulic pressure in RO, and the energy consumption in the RO plant is higher than the energy generated by the PRO plant. In contrast, without the solar PV power, the stand-alone feasibility of a RO desalination plant with osmotic energy generation by the PRO plant can be realized by operating it at a lower water recovery ratio [45]. In such an operation, the energy consumption by the RO plant is fully covered by the energy generation of the PRO plant. As illustrated in Fig. 2(b), at the limiting condition of the SRO operation, the area 3-D-1-2 equals to the area 0-5-4-D.

2.2. RO and PRO membrane process

In the SSRO operation during daytime, the RO desalination is powered by both the PV array and the PRO plant. According to equation (1), the overall energy surplus should be non-negative in order to operate the hybrid system stand-alone. With negligible pressure drop along the membrane

channels in both RO and PRO plants [41, 42], the energy generated by PRO, E_{PRO}, can be represented by the area O-5-4-B, which is

$$E_{PRO} = S_{O-5-4-B} = (Q_{CW} + \Delta Q)\Delta P_{PRO} \tag{2}$$

where Q_{CW} is the volumetric flow rate of the CW, ΔQ is the volumetric flow rate of water permeation in the transportation, ΔP_{PRO} is the hydraulic pressure applied on the CW. In addition, considering the hydraulic energy recovery by the ERD, the energy consumption by the RO plant can be expressed by the area O-0-1-2-3-B, as,

$$W_{RO} = S_{O-0-1-C} - S_{B-3-2-C} = Q_{SW}\Delta P_{RO} - Q_{CW}(\Delta P_{RO} - \Delta P_{PRO}) \tag{3}$$

where Q_{SW} is the volumetric flow rate of the SW and ΔP_{RO} is the applied hydraulic pressure on the SW. As discussed above, in order to operate the hybrid plant stand-alone by the SSRO and SRO schemes, the energy surplus should be non-negative at each operation.

In a RO plant, TR is the limiting operation close to the minimum level of applied pressure (i.e. pressure approaching the concentrated water osmotic pressure plus frictional pressure losses). With the current generation of high permeable RO membrane, it is feasible to operate the RO plant over a wide range of water recoveries to the limit of TR [59]. Zhu has developed a systematic steady-state model of RO operated at TR [59-61] which is used to simulate the performance of the RO plant in this study. In the TR operation of a RO plant, the applied pressure on the feed solution equals the osmotic pressure of the brine at the outlet of the RO membrane module [59], which can be expressed as,

$$\Delta P_{RO} = \frac{\pi_{SW}}{1-Y} = \frac{C_{van't} c_{SW}}{1-Y} \tag{4}$$

where π_{SW} is the osmotic pressure of the SW, $C_{van't}$ is the osmotic pressure coefficient and c_{SW} is the concentration of the SW. It is noted that the van't Hoff law is restricted to use on dilute, ideal solutions [41, 42]. In the salinity range of 0-70 g/kg, the amended linear osmotic pressure coefficient 0.7345 bar·kg·g^{-1} is validated and the maximum deviation is 6.8% [41, 42].

For a constant pressure PRO process (C-PRO), with enough membrane area available (allowable for full-scale PRO discharge), the applied pressure on the draw solution of the PRO process determines the termination of water permeation. This means that the water permeation terminates when the net driving force of the water permeation between the two sides of the membrane is zero [35], which is

$$\Delta P_{PRO} = \Delta \pi_{Outlet} \tag{5}$$

where $\Delta \pi_{Outlet}$ is the osmotic pressure difference at the outlets. For a co-current PRO process, because both the draw and feed solution flow towards the same direction, only one outlet needs to be considered. In contrast, for a counter-current PRO process, with a different pressure applied, the net driving force at either of the two outlets may satisfy the condition and terminate the water permeation. Usually, the counter-current scheme performs better than the co-current scheme due to its high effectiveness [42]. For simplicity, the co-current PRO process is considered first.

In this investigation, the feed water desalinated by the RO system is assumed as SW with 35 g/kg salinity and its osmotic pressure can be obtained according to the van't Hoff's law [41, 42]. Thus, without the consideration of the RSP, based on the mass balance, the osmotic pressure difference at the outlet of the membrane can be expressed as [35],

$$\Delta\pi_{Outlet} = C_{van't}(c_{CW}^{Out} - c_{IW}^{Out}) = C_{van't}\left(\frac{c_{CW}\, q_{CW}}{q_{CW} + \Delta q} - \frac{c_{IW}\, q_{IW}}{q_{IW} - \Delta q}\right) \quad (6)$$

where c_{CW}^{Out} is the concentration of the CW at outlet, c_{IW} and c_{IW}^{Out} are the concentration of the IW at the inlet and outlet, respectively. q_{CW} and q_{IW} are the inlet mass flow rate of the CW and the IW. The inlet flow rate of draw solution is the flow rate of the CW water from the RO system with leakage assumed to be negligible. With 100% salt rejection RO membrane, the concentration of the CW is determined by the water recovery that is $c_{CW} = c_{SW}/(1-Y)$. Δq is flow rate of water permeation across the PRO membrane.

However, in a real PRO process, it is inevitable that the salt permeates from the draw side to the feed side and the performance of the PRO salinity power generation is significantly changed. If the CP effect is considered, the flow rate of the permeation also changes. When these effects are considered, the mass balance is changed to

$$\Delta\pi_{Outlet} = C_{van't}\left(\frac{c_{CW}\, q_{CW} - \Delta S}{q_{CW} + \Delta q_S} - \frac{c_{IW}\, q_{IW} + \Delta S}{q_{IW} - \Delta q_S}\right) \quad (7)$$

where ΔS is the mass rate of the reverse solute, Δq_S is flow rate of water permeation across the PRO membrane considering CP and RSP effects.

The mathematical models and the framework for modelling a process considering the CP and RSP effects are presented in our previous investigation [62]. Generally, during the mass transfer in a real PRO, the water permeates across the membrane. On one hand, the feed solutes are selectively retained by the active layer and accumulated in the support layer, resulting ICP. On the other hand, the permeated water dilutes the draw solution near another side of membrane active layer and causes ECP. In addition, RSP exists because of the non-perfect rejection of the current PRO membrane. Previous studies have developed water flux and solute flux equations for real PRO and have validated these models with experimental results [35, 63]. The steady-state model of the PRO has been demonstrated successfully considering these detrimental effects and describing the reduced water flux and inevitable reverse solute flux. According to the model, reduced water flux, J_W, can be expressed as

$$J_W = A\left(C_{os}\left(\frac{c_D^{PRO}\exp(-J_W/k) - c_F^{PRO}\exp(J_W S/D)}{1 + \frac{B}{J_W}(\exp(J_W S/D) - \exp(-J_W/k))}\right) - \Delta P_{PRO}\right) \quad (8)$$

where A is the membrane water permeability coefficient, B is the membrane solute permeability coefficient. c_D^{PRO} and c_F^{PRO} are the concentration of the PRO draw and the PRO feed, respectively. D is the bulk diffusion coefficient, $k = D/\delta$ is the boundary layer mass transfer coefficient in which δ is the boundary layer thickness, and $S = t_s\tau/\varepsilon$ is the support layer structural parameter in which t_s is the thickness of the porous layer, τ and ε are the tortuosity and porosity of the support layer of the membrane respectively. In addition, the reverse solute flux is

$$J_S = B\left(\frac{c_D^{PRO}\exp(-J_W/k) - c_F^{PRO}\exp(J_W S/D)}{1 + \frac{B}{J_W}(\exp(J_W S/D) - \exp(-J_W/k))}\right) \quad (9)$$

where J_S is the reverse solute flux.

Three sets of experimental data from literature are selected to validate the transport equation of water flux represented in equation (8). The membrane parameters used in the validation are shown in Table 1. Power density, W , is another important membrane characteristic which is the product of the water flux and the operating pressure. For the validation of water flux, the closely related power density is also compared with the experimental results.

In the comparisons, two membranes with different properties are selected. With the first membrane, two different salinity gradients are used, in which feed solution are river water (RW) with concentration 0.9 mM and brackish water (BW) with concentration 80 mM, respectively. The validations of the PRO model are shown in Fig. 3. The results clearly indicate the satisfactory agreement between the modelling results and the experimental results in all the conditions, including the mixing of different salinity gradients and the utilization of different membrane properties.

Furthermore, due to limited experiments of scale-up PRO plant available in the literature, it is difficult to verify the modelled process performance by the experimental results. Thus, modelling a full-scale PRO process using the validated transport equation can be used to determine the viability of real systems and inform their design and operation [64]. In this study, considering the detrimental effects of CP and RSP in salinity power generation, the flow rates of water permeation (Δq_S) and solute permeation (ΔS) is obtained by integrating water flux (J_W) and solute flux (J_S) along the membrane from the inlet to the outlet until the balance as shown equation (5) is established. Detailed steps and framework of PRO modelling can be found in [62]. In addition to the validation with the available experimental data of transport flux, the model of the scale-up PRO process is also validated with the published simulation work. Based on the membrane parameters from [64] which are A 3 $\mathrm{L \cdot m^{-2} \cdot h^{-1} \cdot bar^{-1}}$, B 0.36 $\mathrm{L \cdot m^{-2} \cdot h^{-1}}$ and S 100 μm, and the salinity gradients of draw solution 0.6 M and feed solution 0.015 M, the comparison between the two modelling results of scale-up PRO process are made. Other parameters used in [64] are specific membrane scale (membrane area per 1 $\mathrm{L \cdot h^{-1}}$ initial feed solution) 0.2 $\mathrm{m^2 \cdot (L \cdot h^{-1})^{-1}}$, temperature 298 K, and gas constant 8.314 $\mathrm{J \cdot K^{-1} \cdot mol^{-1}}$. The osmotic pressure is estimated based on the van't Hoff's law which is the product of number of ion species, temperature and gas constant. The comparison is shown in Fig. 4 in which the changing flow rate and concentration of the draw and feed along the flow channels are plotted in a scale-up PRO process. According to [64], the flow rates are converted into the normalized value which is divided by the sum of initial flow rate of the draw and feed solution. As seen in Fig. 4, it is clear that the results simulated based on the modelling framework in this study are in agreement with the modelled results from [64]. In the scale-up PRO process, both the changing flow rates and the concentration are relatively close. Thus, along with the theoretical steady-state model of RO, the overall performance of the hybrid system can be evaluated.

2.3. Solar PV array

Datasheets of a PV array provide the information of the performance of PV devices with respect to standard test condition (STC), namely irradiation 1,000 W/m^2 with an ambient temperature of 25 ^{o}C (298 K). However, practical PV arrays are not always operated at STC. The performance of a PV array depends on the solar irradiation level and the ambient temperature. In this study, single-diode model of a PV array is used to find the non-linear current-voltage equation with the parameters from the product datasheet. In the single-diode PV model, the effect of the series and parallel resistances

are considered and it is warranted that the maximum power of the model matches with the maximum power of the real array [65]. The current-voltage ($I-V$) characteristics of the single-diode PV cell is given by [66]

$$I = I_{PV} - I_0[\exp(\frac{\mathrm{V}+\mathrm{R}_S I}{V_t a})-1] - \frac{V+R_S I}{R_P} \quad (10)$$

where I_{PV} and I_0 are the PV and saturation currents of the array, respectively. V_t is the thermal voltage of the array and is given by $V_t = N_S kT/q$. N_S is the number of cell connected in series, k is the Boltzmann constant (1.3806503×10^{-23} J/K), q is electron charge (1.60217646×10^{-19} C), T is the temperature. R_S and R_P are the equivalent series and the parallel resistance of the array, respectively. Detailed derivation and numerical algorithm to adjust the $I-V$ mode can be found in [65]. The technical data of solar array Bosch M2453BB used in this work is listed in Table 2.

3. Stand-alone salinity-solar power driven RO desalination plant

3.1. Stand-alone solar PV powered RO desalination plant

Works investigating the SEC in steady-state operation of the RO plant are available in the literature [67-69]. But different from the RO plants powered by the electric grid in which the power input is constant, PV powered RO plants are operated along a large variety of power supplies subject to the availability of intermittent solar energy. To deal with the intermittent power input, operation of the RO plant is needed to change for the high effectiveness. The SEC performance of the RO plant has been investigated in previous studies [67, 69]. The outcomes of the SEC of the RO plant operated at TR with hydraulic energy recovery are shown in Fig. 5(a) in which three sets of the efficiencies of devices in the RO plant are considered, including the HP and the ERD.

The inefficiency of the devices shifts the monotonically ideal SEC profile and the inefficiency increase of the devices increases the SEC. In the ideal case with devices of 100% efficiency, the lowest SEC occurs and the SEC increases with the increase of the water recovery in all the range of the ratio studied. In contrast, in the cases with real devices which are not 100% efficient, the profile of the SEC has a minimum among the water recovery ratio. The reason is that at very low water recovery, the energy loss due to the inefficient HP and ERD is relatively large. And hence, the optimum SEC moves to the high water recovery ratio. For instance, the solid line representing the HP efficiency 85% and the ERD efficiency 95% has the optimum SEC approximately 1.3 in the water recovery around 0.18. Actually, the TR operation is the limiting case when the high permeable membrane or/and sufficient area of the membrane is used. In practice, the higher SEC is required when the operation of the RO plant does not meet the thermodynamic restriction (non-TR). For instance, based on the ε-MTU model of the RO plant, with the membrane permeability 3.61×10^{-6} $\cdot kg\cdot m^{-2}\cdot kPa^{-1}\cdot s^{-1}$, flow rate of feed solution 1 $kg\cdot s^{-1}$, and area 100, 200 and 300 m^2, the SEC is presented in Fig. 5(b). The efficiency of the HP is 90%, and efficiency of the ERD is 98%.

In Fig. 5(b), the results clearly indicate that the profiles of the SEC are different with different areas. For areas 100, 200 and 300 m^2, less the area requires, more the SEC in RO desalination. The optimums of the SEC are shifted towards the lower water recovery ratio with the decrease on the membrane area. In addition, comparing the profile of area 300 m^2 with the SEC profile of a TR RO plant in Fig. 5(a) with the devices with same efficiency, it is found that the profile of area 300 m^2

approximately have the same values in all the range of water recovery. Consequently, in this case, with the usage of 300 m^2 area, the TR operation of the RO can be achieved.

Based on the results shown in Fig.5, with different parameters (conditions and usages of devices and membrane), the RO plant performs differently. But at each fixed condition, a minimum SEC can be found, thus the RO plant can be operated optimally. To this end, to deal with the variable load from the solar PV array, the flow rate of the feed solution can be adjusted to ensure that the RO plant is operated most efficiently with respect to energy consumption. Thus, in a PVRO plant (operation with TR and non-TR), with certain power supply from the solar PV array, the maximum water production rate can be expressed as

$$q_P^{MAX} = \frac{E_{PV}}{SEC^{MIN}} \tag{11}$$

where SEC^{MIN} denotes the minimum SEC of the RO plant and q_P^{MAX} is the maximum water production under certain solar energy supply, E_{PV} .

Previous studies have investigated the operation of RO plants under variable-load and suggested that the RO desalination plant can operate successfully under varying flow rate and pressure without any technical problems [15, 16]. In addition, it has been pointed out that relatively short time is needed for the transition from one steady state to another steady state for a RO process and the pseudo steady-state model can be assumed for time steps more than 0.25 h [70]. Therefore, it is practical to study the RO plant in this work with the hourly data of solar irradiation and ambient temperature. In this work the optimal strategy of the PVRO plant is to control the flow rate of the feed solution (CW) and the pressure, ensuring that the RO plant is operated at the available minimum SEC state.

3.2. Dynamics of the hybrid RO-PRO system

When the osmotic energy recovery is considered in the RO desalination plant, the net SEC (SEC_{net}) that is the overall SEC considering the specific energy generation in the PRO plant, can be expressed as

$$SEC_{net} = \frac{W_{RO} - E_{PRO}}{Q_{PW}} \tag{12}$$

where Q_{PW} is the volumetric flow rate of the PW. Based on equations of energy consumed by the RO plant and energy generated by the PRO, the net SEC can be obtained. In the salinity energy harvesting by the PRO, the CP and RSP cannot be avoided in real applications. As a result, with the reduced energy generation in the PRO, the net SEC is increased. According to the framework of simulating the CP and RSP effect in salinity energy generation [62], the net SEC considering the overall detrimental effects in the PRO plant and the reduced performance can also be obtained. The results of the optimum net SEC of the RO desalination plant with the osmotic energy generation are presented in Fig. 6(a). The optimum net SEC of the RO-PRO plant without the CP and RSP is obtained through the maximum salinity energy harvest from the mixture of CW and IW by applying the optimum hydraulic pressure on the CW [35]. The optimum net SEC of the RO-PRO plant considering the CP and RSP effects is numerically obtained. The parameters used in the simulations of the salinity power harvest by the PRO are: water permeability 1.74 L $m^{-2}\cdot h^{-1}bar^{-1}$, salt permeability 0.16 L $m^{-2}\cdot h^{-1}$,

and structural parameter 307 μm, temperature 298 K, mass transfer coefficient 138.6 $L \cdot m^{-2} h^{-1}$ [63], diffusion coefficient 1.49×10^{-9} $m^2 \cdot s^{-1}$ [71], and van't Hoff coefficient 0.7345 $bar \cdot kg \cdot g^{-1}$ [42]. The efficiency of the HP is 90%, efficiency of the ERD is 98% and efficiency of the HT is 90%.

The results clearly indicate that the optimum net SEC of RO desalination with osmotic energy recovery by the PRO is significantly decreased compared to that of the SEC of the RO plant without osmotic energy recovery. Furthermore, the detrimental effects raise the optimum net SEC in all studied RO operations. Considering the CP and RSP effects, less the osmotic energy is generated from the PRO plant, more the net SEC is required.

At the lower range of the water recovery, the negative net SEC indicates that the salinity power generated by the PRO is larger than the energy consumed by the RO. Therefore, the operations at RO water recovery ratios with non-positive optimum net SEC are the feasible operations for the SRO operation of the hybrid plant. In Fig. 6(a), the feasible operational window for the SRO operation is O-B-E-C and considering the detrimental effects the feasible operational window becomes O-A-D-C. Moreover, with the increase of the RO water recovery, the optimum net SEC increases as well. In the range of the water recovery ratio with positive optimum net SEC, the osmotic energy generated by the PRO cannot fully cover the energy consumed by the RO desalination. The power shortage can be supplemented by the energy from solar PV array in the proposed hybrid system. Thus, these RO water recovery ratios belong to the SSRO operation. Under the constrained range of the RO water recovery, from 0.1 to 0.5, in Fig. 6(a), the maximum feasible operational window of the SSRO operation is restricted by the window E-F-H-G for the ideal PRO salinity harvest and by the window D-F-J-I for the PRO salinity harvest considering the CP and RSP effects.

The upper and lower limits of the feasible operational windows are determined by different factors in the two operational schemes. In the feasible operational window of the SRO operation, the lower limits of both operations with or without the CP and RSP effects are restricted by the lowest RO water recovery ratio. But the upper limits are different due to the performance limiting effects. The upper limit is significantly decreased when the CP and RSP effects are considered. Conversely, theoretically the lower limit of the SSRO operation is the upper limit of the SRO operation in both cases. The upper limit depends on the specific available solar power per unit production water, $e_{PV} = E_{PV} / V_{PW}$. If the required water recovery by the specific available solar power is lower than the maximum water recovery ratio studied (0.5), the upper limit of the SSRO operation is the required water recovery ratio by the specific available solar power. Otherwise, with the enough energy from the PV array, the upper limit is restricted by the maximum water recovery 0.5. One specific SSRO operation with a certain specific solar power is illustrated in Fig. 6(b). The upper limit of the RO water recovery is less than 0.5, namely state A for the PRO salinity extraction considering the CP and RSP effects and state B for the ideal PRO salinity extraction.

Actually, similar to the PVRO plant, the water is needed to be optimally produced by the PVROPRO plant. The optimum operation of the SRO and SSRO schemes are achieved at their upper limits of the RO water recovery ratio. From the perspective of the optimum operation, the detrimental effects reduce the upper limit of the RO water recovery ratio in both the SRO and SSRO schemes. In Fig. 6(a), in the window of the SRO operation, the optimum operation of the RO with ideal PRO power generation is the state E, whilst the optimum is state D due to the real CP and RSP effects. In the SSRO operational window, under certain specific available solar power (e_{PV}), the upper limit is also further restricted by the detrimental effects as illustrated in Fig. 6(b). The optimum operation of the RO with ideal PRO power generation is the state B. In contrast, the optimum ratio is reduced to state A due to the real CP and RSP effects. The resulting lower maximum water recovery

ratio, accordingly, causes the lower water production rate at the constant flow rate of the SW or the higher required flow rate of the SW to produce a certain volume of the PW.

3.3. Simulation framework of the stand-alone salinity-solar power driven RO desalination plant

A flow chart illustrating the simulation framework is shown in Fig. 7. In order to simulate the PVROPRO hybrid power desalination plant, several inputs are needed, including the input parameters of the system and the environmental data of solar and salinity. The input parameters of the PV array are the efficiency of the PV panel which is 15% and the number of the PV panels which is 20. The parameters of the PRO membrane are the same as that in Section 3.2. The RO plant is assumed to be operated at the TR operation. The yearly data of solar irradiation and ambient temperature of Perth, Australia is provided by Meteonorm 7 software [72] and used in this study for a case study of the proposed hybrid power RO desalination plant. The concentration of SW is 35 g/kg and the concentration of the IW is assumed to be 0.1 g/kg.

In the simulation, firstly the performance of the stand-alone PVRO plant is evaluated. The PVRO plant is optimized to find the appropriate flow rate of the SW to ensure the minimum SEC. Then, with the same devices (e.g. HP pumps) within the PV array and the RO plant, the proposed hybrid powered RO desalination plant is modelled. The same pumps implementation denotes that the maximum flow rate in the PVROPRO plant is restricted by the maximum flow rate in the PVRO plant. In the simulation, the solar PV power generation is assumed to be operated with maximum power point tracking that the available maximum power is supplied to the desalination plant under certain environmental condition.

4. Results and analysis

A stand-alone RO desalination plant powered by PV array is first modelled with predefined parameters. The RO plant is operated at its minimum SEC, and then the maximum water production is obtained under certain level of solar PV power based on Equation (11). In addition, with the same scale of flow rate of the SW used in the PVRO plant, the hybrid solar-salinity powered RO desalination plant is modelled. Because the stand-alone feasibility of the hybrid solar-salinity powered RO desalination system depends on the relation between the flow rates of the SW and the IW, another advantage of the PVROPRO plant is that it can be operated at a larger SW flow rate if the volume of IW is sufficient. In this study, the total dimensionless flow rate which is the ratio of the IW flow rate to the sum of the SW and the IW flow rate is assumed as 0.5 in modelling both the processes with and without osmotic energy generation. The flow rate of the SW is selected as the maximum flow rate of the SW required in the stand-alone PVRO plant. Thus, the same flow rate of the IW is required to meet the predefined overall dimensionless flow rate. In both the SSRO and SRO schemes, the maximum RO water recovery ratio can be obtained by solving Equation (1) with the limiting zero overall energy surplus. Moreover, the effects of the CP and RSP are investigated with the same flow operation, namely the flow rate of the SW and the IW.

4.1. Overall optimum production rates of the PW

The objective is to maximize the flow rate of PW in the PVRO and the PVROPRO plants. With hourly PV solar power calculated, both the SSRO and SRO operations are optimised. During the search, with the step-size of the RO water recovery ratio 0.01 (1%), all the operations in the range of RO water recovery (0.1 – 0.5) are calculated and compared. Then, the hourly optimum RO operation for the maximum water production is obtained. The results, as presented in Fig. 8, show the increased water production by the osmotic power generation and the water reduction due to the CP and RSP effects. These two influences are represented by the relative PW increase and decrease, respectively, which are defined as

$$q_{PW}^{+} = \frac{q_{PW}^{PVROPRO} - q_{PW}^{PVRO}}{q_{PW}^{PVRO}};$$
$$q_{PW}^{-} = \frac{q_{PW}^{PVROPRO} - q_{PW}^{PVROPRO,CPRSP}}{q_{PW}^{PVROPRO}} \quad (13)$$

where q_{PW}^{+} and q_{PW}^{-} are the relative PW increase due to osmotic energy generation and the relative water decrease due to the CP and RSP effects in PRO salinity power harvest, respectively. q_{PW}^{PVRO}, $q_{PW}^{PVROPRO}$, and $q_{PW}^{PVROPRO,CPRSP}$ are the flow rates of the PW in the stand-alone PVRO plant and the stand-alone PVROPRO plant with and without the detrimental effects.

The results clearly indicate the dependence of the PW flow rate on the available PV solar power. The water production rate varies with respect to different solar power availability in both the PVRO and PVROPRO plants. However, with the salinity power generation, the PW water production rate is considerably increased and less fluctuated. Comparing Fig. 8(a) and 8(b), the hourly production rate of the PVROPRO plant is much larger than that of the PVRO plant. In the PVROPRO plant, due to the salinity power generation, the desalination plant can be operated continuously. In the SRO operation, a constant water production is achievable at the upper limit of the RO water recovery as shown in Fig. 6(a) (state E). In addition, during daytime, with the available solar power, more PW can be treated in the stand-alone desalination plant as illustrated in Fig. 6(b) (state B). The relative PW increase is presented in Fig. 8(c) with respect to weekly PW production. The results show significant increase in PW production due to incorporation of the salinity power harvesting technology in the PVRO desalination plant. It is observed in Fig. 8(c) that, the PW production rate of the most improved week is almost 20 times the rate in PVRO plant. On average, the yearly PW production of the PVROPRO plant is increased more than nine times the stand-alone PVRO plant. Furthermore, the profile of the relative PW production increase shows that the more increase occurs when the PW rate in the PVRO plant are less, i.e. hour 4000 – 5000 in Fig. 8(a) and week 20 – 30 in Fig. 8(c). Because there was less irradiation in magnitude and shorter daytime during such periods in the year, the PV solar power is reduced. Simultaneously, the continuous osmotic power generation which is less periodic, plays a more important role to sustain the plant when the solar PV power is relatively lower.

When the overall performance limiting effects in PRO salinity energy harvest are considered, the salinity power generation decreases. Thus, the overall PW production of the hybrid desalination decreases as well. The weekly relative PW decrease is shown in Fig. 8(d). According to the simulations with the membrane studied, the weekly PW production rates are decreased in the range of 16-20%. Annually, the overall PW production is reduced by 18.07% due to the CP and RSP effects. In addition, it is found that the most significant reduction also occurs when the solar power is less. In the SSRO operation, the optimum RO water recovery ratio is lower when the solar power is less. And

for the proposed hybrid desalination plant, lower RO water recovery rate causes more energy loss due to the detrimental effects. As shown in Fig. 6(b), with the increase of the RO water recovery rate, the deviation between the two dotted lines become less at the same water recovery rate. Therefore, during the period with less solar irradiation, more reduction due to the CP and RSP effect may result in.

4.2. Optimum operations of the stand-alone RO desalination plant

The optimum operation of the stand-alone RO desalination plants is studied, including the stand-alone PVRO plant and the stand-alone PVROPRO plant with and without consideration of the detrimental effects. The optimum flow rate of the SW and the optimum water recovery ratio are shown in Fig. 9. A summer day with 24 hours (from the 25^{th} to 48^{th} hours, as shown in Fig. 8), is considered to compare the different optimum operation of the stand-alone RO desalination plant.

The results clearly indicate different optimum operation required for the two RO desalination plants. The SW flow rate of the PVRO plant clearly indicates the varying optimum flow rate with respect to the available solar power. In the range of hours without solar power (hour 1-5 and hour 21-24), the flow rate of the SW are zero and also zero treated freshwater is produced. In contrast, during daytime, the flow rate is changed in order to ensure the RO plant operated at its minimum SEC operation as shown in Fig. 9(b). The optimum water recovery ratio of the PVRO plant is 0.13. It can be controlled by the hydraulic pressure applied on the SW based on the TR condition.

Conversely, the simulations of the PVROPRO plant are developed with the constant flow rate of the SW as presented in Fig. 9(a). All the flow rates during a day are constant. In the PVROPRO plant, the flow rate of the SW is selected as the maximum in the PVRO plant for the entire year. With the osmotic energy generation by the PRO plant, the RO desalination plant can be operated consecutively over night at a low water recovery, as shown in Fig. 9(b). However, the performance limiting effects reduce the optimum water recovery ratio in both the SSRO and SRO operation. In Fig. 9(b), the optimum states discussed in Fig. 6 can be identified in the 24 hours operation. It is noted that the PVROPRO without the CP and RSP effects, operation of hours 1-5 and hours 21-24, is carried out at the state E shown in Fig. 6(a), and operation of hours 6-20 is carried out at the state B shown in Fig. 6(b) subject to different solar power. In addition, when the CP and RSP effects are considered, operation of hours 1-5 and hours 21-24 is carried out at the state D as shown in Fig. 6(a), and operation of hours 6-20 is carried out at the state A as shown in Fig. 6(b).

4.3. Optimum operations of the PRO plant

In the PRO plant, the flow rate of the CW is determined by the RO water recovery ratio in the RO plant. The flow rate of the IW might be restricted by the local condition of the low concentration streams. Because compared to available SW in coastal regions, the availability of low concentration stream is always limited. In this study, the overall dimensionless flow rate is assumed to be 0.5 that the IW flow rate is same to that of the SW. Therefore, in order to extract the maximum salinity energy from the given volume of the SW and the IW, the hydraulic pressure applied on the CW should be optimised. In the ideal PVROPRO plant in which the CP and RSP effects are ignored, the maximum osmotic energy extraction can be analytically obtained [35]. But for a PRO plant with the

CP and RSP effects considered, the maximum extractable energy cannot be easily calculated. It needs simulation by certain step-size of the pressure and comparison between the results to search for the optimum [62]. With different membrane used (water and salt permeability coefficients, structural parameter, and et al.) and flow parameters (flow rates, flow directions et al.), the phenomena and detrimental effects of the CP and RSP are different. Based on the membrane and flow parameters in this study, the results of the optimum operations are shown in Fig. 10 in which both the PVROPRO plant with and without consideration of the CP and RSP effects are included.

The results indicate the optimum operational widow during a day subject to the availability of solar power. Higher hydraulic pressure is required during daytime for both PVROPRO plants. It is a result of the more concentrated CW caused by the higher water recovery in the RO plant with the PV array in operation. Moreover, the overall detrimental effect on the optimum applied pressure is also studied. The results show that, when the CP and RSP effects are considered, the required optimum pressure is lower in both the SSRO and SRO operation, which is a result of the reduced osmotic energy generation.

5. Conclusions

An investigation into the development of a novel stand-alone RO seawater desalination plant powered by a solar PV and a PRO is carried out. Two stand-alone schemes, the SSRO and SRO operation, are proposed and investigated using a state-diagram. With the mathematical models describing the membrane process of the RO, the PRO and the solar PV energy harvest, the stand-alone feasibility is studied numerically and both the feasible operational windows of the SSRO and SRO operation are analysed. In addition, the detrimental effects, the CP and the RSP, are also investigated. Finally, with the hourly solar data of Perth, Australia in a year, the production rates of the PVROPRO plant during a year is modelled and the optimum operational widows are identified and discussed. Based on the results, some conclusions can be drawn: 1) the feasibility of the PVROPRO plant can be realized by the SSRO operation during the daytime and by the SRO operation over night when sun is unavailable; 2) the operational windows are identified in the case of both the SRO and SSRO operation in the PVROPRO plant, and the upper limit in each operational window is the optimum operation; 3) the production rate is significantly increased by the integration of the salinity power generation by the PRO plant. The highest weekly production rate of the PVROPRO plant is almost 20 times the rate in PVRO at the same week. Annual production of the PVROPRO plant is increased more than nine times that of the stand-alone PVRO plant; 4) the CP and RSP effects in the PRO plant reduce the performance of the PVROPRO plant. The weekly PW production rate is decreased in the range of 16-20% due to the detrimental effects. Annually, the overall production is reduced by 18.07%.

References

[1] S.A. Kalogirou, Seawater desalination using renewable energy sources, Progress in Energy and Combustion Science, 31 (2005) 242-281.
[2] M.A. Shannon, P.W. Bohn, M. Elimelech, J.G. Georgiadis, B.J. Marinas, A.M. Mayes, Science and technology for water purification in the coming decades, Nature, 452 (2008) 301-310.
[3] C. Fritzmann, J. Löwenberg, T. Wintgens, T. Melin, State-of-the-art of reverse osmosis desalination, Desalination, 216 (2007) 1-76.
[4] A. Subramani, M. Badruzzaman, J. Oppenheimer, J.G. Jacangelo, Energy minimization strategies and renewable energy utilization for desalination: A review, Water Research, 45 (2011) 1907-1920.

[5] A. Al-Karaghouli, D. Renne, L.L. Kazmerski, Solar and wind opportunities for water desalination in the Arab regions, Renewable and Sustainable Energy Reviews, 13 (2009) 2397-2407.
[6] H. Doukas, K.D. Patlitzianas, A.G. Kagiannas, J. Psarras, Renewable energy sources and rationale use of energy development in the countries of GCC: Myth or reality?, Renewable Energy, 31 (2006) 755-770.
[7] E.M.A. Mokheimer, A.Z. Sahin, A. Al-Sharafi, A.I. Ali, Modeling and optimization of hybrid wind–solar-powered reverse osmosis water desalination system in Saudi Arabia, Energy Conversion and Management, 75 (2013) 86-97.
[8] G.H. Xia, Q.X. Sun, X. Cao, J.F. Wang, Y.Z. Yu, L.S. Wang, Thermodynamic analysis and optimization of a solar-powered transcritical CO2 (carbon dioxide) power cycle for reverse osmosis desalination based on the recovery of cryogenic energy of LNG (liquefied natural gas), Energy, 66 (2014) 643-653.
[9] E. Antipova, D. Boer, L.F. Cabeza, G. Guillén-Gosálbez, L. Jiménez, Uncovering relationships between environmental metrics in the multi-objective optimization of energy systems: A case study of a thermal solar Rankine reverse osmosis desalination plant, Energy, 51 (2013) 50-60.
[10] A.M. Blanco-Marigorta, M. Masi, G. Manfrida, Exergo-environmental analysis of a reverse osmosis desalination plant in Gran Canaria, Energy, 76 (2014) 223-232.
[11] F. Calise, M.D. d'Accadia, A. Piacentino, A novel solar trigeneration system integrating PVT (photovoltaic/ thermal collectors) and SW (seawater) desalination: Dynamic simulation and economic assessment, Energy, 67 (2014) 129-148.
[12] R.S. El-Emam, I. Dincer, Thermodynamic and thermoeconomic analyses of seawater reverse osmosis desalination plant with energy recovery, Energy, 64 (2014) 154-163.
[13] A. Ghobeity, A. Mitsos, Optimal time-dependent operation of seawater reverse osmosis, Desalination, 263 (2010) 76-88.
[14] P.C.M. de Carvalho, D.B. Riffel, C. Freire, F.F.D. Montenegro, The Brazilian experience with a photovoltaic powered reverse osmosis plant, Progress in Photovoltaics: Research and Applications, 12 (2004) 373-385.
[15] M. Thomson, M.S. Miranda, D. Infield, A small-scale seawater reverse-osmosis system with excellent energy efficiency over a wide operating range, Desalination, 153 (2003) 229-236.
[16] M. Thomson, D. Infield, A photovoltaic-powered seawater reverse-osmosis system without batteries, Desalination, 153 (2003) 1-8.
[17] A. Joyce, D. Loureiro, C. Rodrigues, S. Castro, Small reverse osmosis units using PV systems for water purification in rural places, Desalination, 137 (2001) 39-44.
[18] H.Ş. Aybar, J.S. Akhatov, N.R. Avezova, A.S. Halimov, Solar powered RO desalination: Investigations on pilot project of PV powered RO desalination system, Appl. Sol. Energy, 46 (2010) 275-284.
[19] A.M. Bilton, L.C. Kelley, S. Dubowsky, Photovoltaic reverse osmosis — Feasibility and a pathway to develop technology, Desalination and Water Treatment, 31 (2011) 24-34.
[20] A.M. Bilton, R. Wiesman, A.F.M. Arif, S.M. Zubair, S. Dubowsky, On the feasibility of community-scale photovoltaic-powered reverse osmosis desalination systems for remote locations, Renewable Energy, 36 (2011) 3246-3256.
[21] N. Fraidenraich, O.C. Vilela, G.A. Lima, Specific energy consumption of PV reverse osmosis systems. Experiment and theory, Progress in Photovoltaics: Research and Applications, 21 (2013) 612-619.
[22] A. Poullikkas, An optimization model for the production of desalinated water using photovoltaic systems, Desalination, 258 (2010) 100-105.
[23] L.C. Kelley, S. Dubowsky, Thermal control to maximize photovoltaic powered reverse osmosis desalination systems productivity, Desalination, 314 (2013) 10-19.
[24] A. Ben Chaabene, A. Sellami, A novel control of a Reverse Osmosis Desalination system powered by photovoltaic generator, in: Electrical Engineering and Software Applications (ICEESA), 2013 International Conference on, 2013, pp. 1-6.

[25] J.T. Bialasiewicz, Renewable Energy Systems With Photovoltaic Power Generators: Operation and Modeling, Industrial Electronics, IEEE Transactions on, 55 (2008) 2752-2758.
[26] D. Ipsakis, S. Voutetakis, P. Seferlis, F. Stergiopoulos, C. Elmasides, Power management strategies for a stand-alone power system using renewable energy sources and hydrogen storage, International Journal of Hydrogen Energy, 34 (2009) 7081-7095.
[27] G. Bekele, G. Tadesse, Feasibility study of small Hydro/PV/Wind hybrid system for off-grid rural electrification in Ethiopia, Applied Energy, 97 (2012) 5-15.
[28] H. Cherif, J. Belhadj, Large-scale time evaluation for energy estimation of stand-alone hybrid photovoltaic-wind system feeding a reverse osmosis desalination unit, Energy, 36 (2011) 6058-6067.
[29] T. Novosel, B. Ćosić, G. Krajačić, N. Duić, T. Pukšec, M. Mohsen, M. Ashhab, A. Ababneh, The influence of reverse osmosis desalination in a combination with pump storage on the penetration of wind and PV energy: A case study for Jordan, Energy, 76 (2014) 73-81.
[30] B.E. Logan, M. Elimelech, Membrane-based processes for sustainable power generation using water, Nature, 488 (2012) 313-319.
[31] W. He, Y. Wang, M.H. Shaheed, Energy and thermodynamic analysis of power generation using a natural salinity gradient based pressure retarded osmosis process, Desalination, 350 (2014) 86-94.
[32] S.E. Skilhagen, Osmotic power — a new, renewable energy source, Desalination and Water Treatment, 15 (2010) 271-278.
[33] A. Achilli, A.E. Childress, Pressure retarded osmosis: From the vision of Sidney Loeb to the first prototype installation — Review, Desalination, 261 (2010) 205-211.
[34] S.E. Skilhagen, J.E. Dugstad, R.J. Aaberg, Osmotic power — power production based on the osmotic pressure difference between waters with varying salt gradients, Desalination, 220 (2008) 476-482.
[35] N.Y. Yip, M. Elimelech, Thermodynamic and Energy Efficiency Analysis of Power Generation from Natural Salinity Gradients by Pressure Retarded Osmosis, Environmental Science & Technology, 46 (2012) 5230-5239.
[36] W. He, Y. Wang, M.H. Shaheed, Enhanced energy generation and membrane performance by two-stage pressure retarded osmosis (PRO), Desalination, 359 (2015) 186-199.
[37] Y.C. Kim, M. Elimelech, Potential of osmotic power generation by pressure retarded osmosis using seawater as feed solution: Analysis and experiments, Journal of Membrane Science, 429 (2013) 330-337.
[38] A. Altaee, Zaragoza, Guillermo, Sharif, Adel, Pressure retarded osmosis for power generation and seawater desalination: Performance analysis, Desalination, 344 (2014).
[39] M.H. Sharqawy, S.M. Zubair, J.H. Lienhard V, Second law analysis of reverse osmosis desalination plants: An alternative design using pressure retarded osmosis, Energy, 36 (2011) 6617-6626.
[40] B.J. Feinberg, G.Z. Ramon, E.M.V. Hoek, Thermodynamic Analysis of Osmotic Energy Recovery at a Reverse Osmosis Desalination Plant, Environmental Science & Technology, 47 (2013) 2982-2989.
[41] L.D. Banchik, M.H. Sharqawy, J.H. Lienhard V, Effectiveness-mass transfer units (ε-MTU) model of a reverse osmosis membrane mass exchanger, Journal of Membrane Science, 458 (2014) 189-198.
[42] M.H. Sharqawy, L.D. Banchik, J.H. Lienhard V, Effectiveness–mass transfer units (ε–MTU) model of an ideal pressure retarded osmosis membrane mass exchanger, Journal of Membrane Science, 445 (2013) 211-219.
[43] J.L. Prante, J.A. Ruskowitz, A.E. Childress, A. Achilli, RO-PRO desalination: An integrated low-energy approach to seawater desalination, Applied Energy, 120 (2014) 104-114.
[44] A. Achilli, J.L. Prante, N.T. Hancock, E.B. Maxwell, A.E. Childress, Experimental Results from RO-PRO: A Next Generation System for Low-Energy Desalination, Environmental Science & Technology, 48 (2014) 6437-6443.
[45] W. He, Y. Wang, A. Sharif, M.H. Shaheed, Thermodynamic analysis of a stand-alone reverse osmosis desalination system powered by pressure retarded osmosis, Desalination, 352 (2014) 27-37.
[46] L.D. Banchik, M.H. Sharqawy, J.H. Lienhard V, Limits of power production due to finite membrane area in pressure retarded osmosis, Journal of Membrane Science, 468 (2014) 81-89.

[47] S. van der Zwan, I.W.M. Pothof, B. Blankert, J.I. Bara, Feasibility of osmotic power from a hydrodynamic analysis at module and plant scale, Journal of Membrane Science, 389 (2012) 324-333.
[48] J. Kim, M. Park, S.A. Snyder, J.H. Kim, Reverse osmosis (RO) and pressure retarded osmosis (PRO) hybrid processes: Model-based scenario study, Desalination, 322 (2013) 121-130.
[49] B.J. Feinberg, G.Z. Ramon, E.M.V. Hoek, Scale-up characteristics of membrane-based salinity-gradient power production, Journal of Membrane Science, 476 (2015) 311-320.
[50] H.E. Garcia, A. Mohanty, W.-C. Lin, R.S. Cherry, Dynamic analysis of hybrid energy systems under flexible operation and variable renewable generation – Part I: Dynamic performance analysis, Energy, 52 (2013) 1-16.
[51] H.E. Garcia, A. Mohanty, W.-C. Lin, R.S. Cherry, Dynamic analysis of hybrid energy systems under flexible operation and variable renewable generation – Part II: Dynamic cost analysis, Energy, 52 (2013) 17-26.
[52] M.R. Ali Ehyaei, M.; Ahmadi, Meeting the Electrical Energy Needs of a Residential Building with a Wind-Photovoltaic Hybrid System, in: In Proceedings of the 4th World Sustain. Forum, Sciforum Electronic Conference Series, 2015.
[53] M. Dali, J. Belhadj, X. Roboam, Hybrid solar–wind system with battery storage operating in grid-connected and standalone mode: Control and energy management – Experimental investigation, Energy, 35 (2010) 2587-2595.
[54] H. Ibrahim, R. Younès, T. Basbous, A. Ilinca, M. Dimitrova, Optimization of diesel engine performances for a hybrid wind–diesel system with compressed air energy storage, Energy, 36 (2011) 3079-3091.
[55] M.O. Abdullah, V.C. Yung, M. Anyi, A.K. Othman, K.B. Ab. Hamid, J. Tarawe, Review and comparison study of hybrid diesel/solar/hydro/fuel cell energy schemes for a rural ICT Telecenter, Energy, 35 (2010) 639-646.
[56] W. Qi, J. Liu, P.D. Christofides, A distributed control framework for smart grid development: Energy/water system optimal operation and electric grid integration, Journal of Process Control, 21 (2011) 1504-1516.
[57] W. Qi, J. Liu, P.D. Christofides, Supervisory predictive control for long-term scheduling of an integrated wind/solar energy generation and water desalination system, Control Systems Technology, IEEE Transactions on, 20 (2012) 504-512.
[58] S. Zhang, T.-S. Chung, Minimizing the Instant and Accumulative Effects of Salt Permeability to Sustain Ultrahigh Osmotic Power Density, Environmental Science & Technology, 47 (2013) 10085-10092.
[59] A. Zhu, P.D. Christofides, Y. Cohen, Energy Consumption Optimization of Reverse Osmosis Membrane Water Desalination Subject to Feed Salinity Fluctuation, Industrial & Engineering Chemistry Research, 48 (2009) 9581-9589.
[60] A. Zhu, P.D. Christofides, Y. Cohen, Effect of thermodynamic restriction on energy cost optimization of RO membrane water desalination, Industrial & Engineering Chemistry Research, 48 (2008) 6010-6021.
[61] A. Zhu, P.D. Christofides, Y. Cohen, Minimization of energy consumption for a two-pass membrane desalination: effect of energy recovery, membrane rejection and retentate recycling, Journal of Membrane Science, 339 (2009) 126-137.
[62] W. He, Y. Wang, M.H. Shaheed, Modelling of osmotic energy from natural salt gradients due to pressure retarded osmosis: effects of detrimental factors and flow schemes, Journal of Membrane Science, (2014).
[63] N.Y. Yip, A. Tiraferri, W.A. Phillip, J.D. Schiffman, L.A. Hoover, Y.C. Kim, M. Elimelech, Thin-Film Composite Pressure Retarded Osmosis Membranes for Sustainable Power Generation from Salinity Gradients, Environmental Science & Technology, 45 (2011) 4360-4369.
[64] A.P. Straub, S. Lin, M. Elimelech, Module-Scale Analysis of Pressure Retarded Osmosis: Performance Limitations and Implications for Full-Scale Operation, Environmental Science & Technology, (2014).

[65] M.G. Villalva, J.R. Gazoli, E.R. Filho, Comprehensive Approach to Modeling and Simulation of Photovoltaic Arrays, Power Electronics, IEEE Transactions on, 24 (2009) 1198-1208.
[66] M.G. Villalva, J.R. Gazoli, E.R. Filho, Modeling and circuit-based simulation of photovoltaic arrays, in: Power Electronics Conference, 2009. COBEP '09. Brazilian, 2009, pp. 1244-1254.
[67] A. Zhu, P.D. Christofides, Y. Cohen, Minimization of energy consumption for a two-pass membrane desalination: Effect of energy recovery, membrane rejection and retentate recycling, Journal of Membrane Science, 339 (2009) 126-137.
[68] A.R. Bartman, A. Zhu, P.D. Christofides, Y. Cohen, Minimizing energy consumption in reverse osmosis membrane desalination using optimization-based control, Journal of Process Control, 20 (2010) 1261-1269.
[69] A. Zhu, A. Rahardianto, P.D. Christofides, Y. Cohen, Reverse osmosis desalination with high permeability membranes — Cost optimization and research needs, Desalination and Water Treatment, 15 (2010) 256-266.
[70] K.M. Sassi, I.M. Mujtaba, Optimal operation of RO system with daily variation of freshwater demand and seawater temperature, Computers & Chemical Engineering, 59 (2013) 101-110.
[71] A. Achilli, T.Y. Cath, A.E. Childress, Power generation with pressure retarded osmosis: An experimental and theoretical investigation, Journal of Membrane Science, 343 (2009) 42-52.
[72] Meteonorm Software 7 (http://meteonorm.com/), in, Access in September 2014.
[73] X. Song, Z. Liu, D.D. Sun, Energy recovery from concentrated seawater brine by thin-film nanofiber composite pressure retarded osmosis membranes with high power density, Energy & Environmental Science, 6 (2013) 1199-1210.
[74] S.C. Chen, C.F. Wan, T.-S. Chung, Enhanced fouling by inorganic and organic foulants on pressure retarded osmosis (PRO) hollow fiber membranes under high pressures, Journal of Membrane Science, 479 (2015) 190-203.

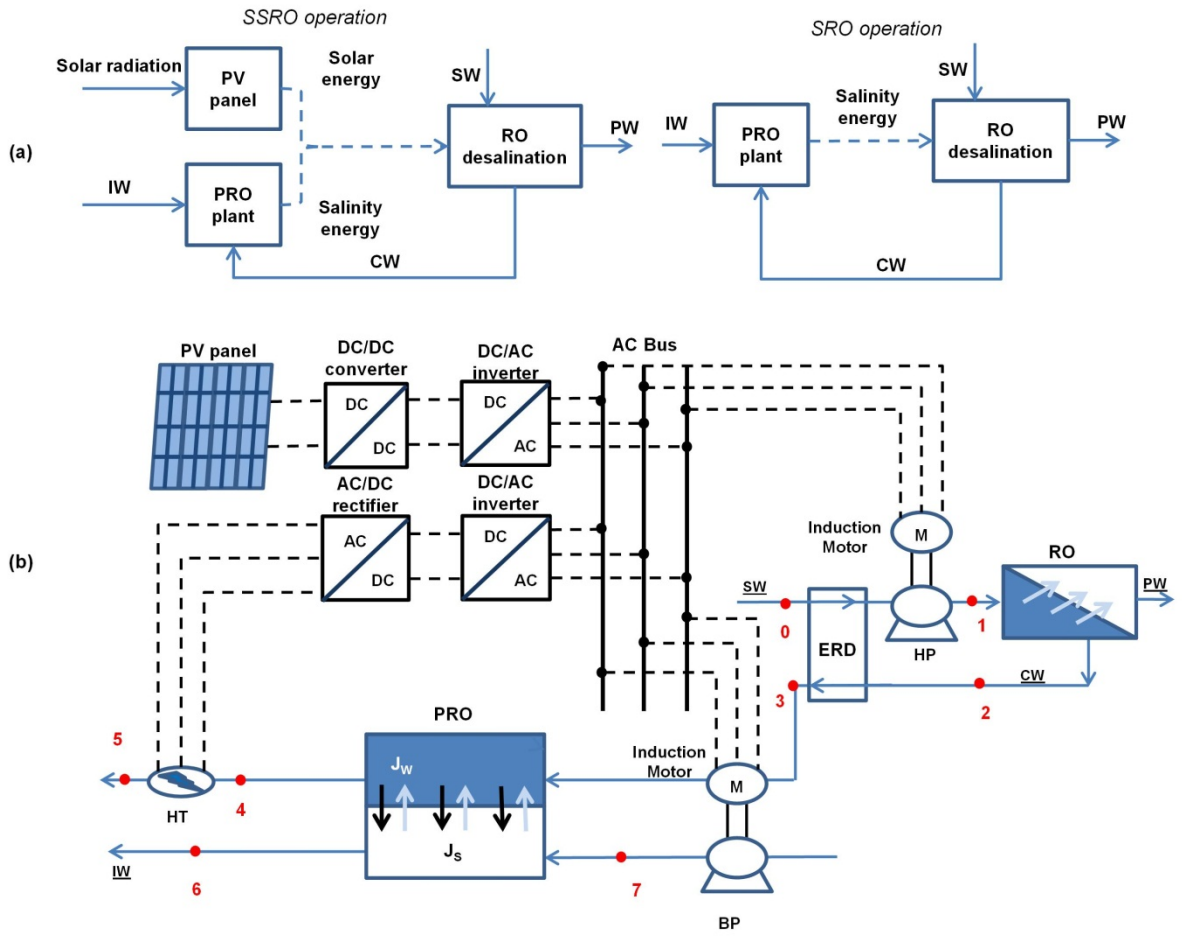

Fig. 1. Illustration of two operations in the proposed solar-salinity power driven RO desalination plant is presented in (a) and schematic diagram of the solar-salinity power driven seawater RO desalination plant is presented in (b).

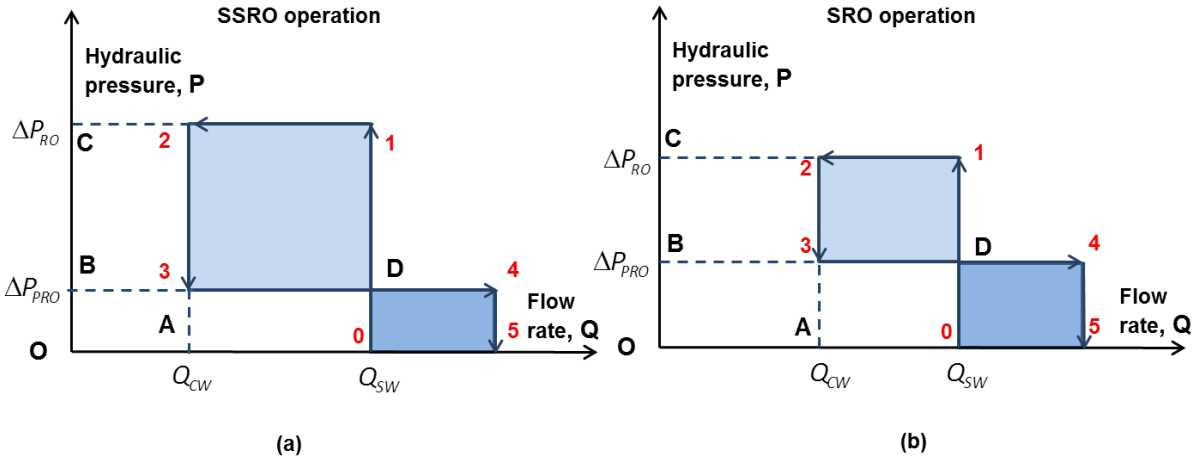

Fig. 2. Thermodynamic analysis of the hybrid salinity-solar power driven RO desalination plant in hydraulic pressure and flow rate diagram, P-Q diagram. In (a), the salinity cycle of the SSRO operation is illustrated, and the cycle of the SRO operation is illustrated in (b).

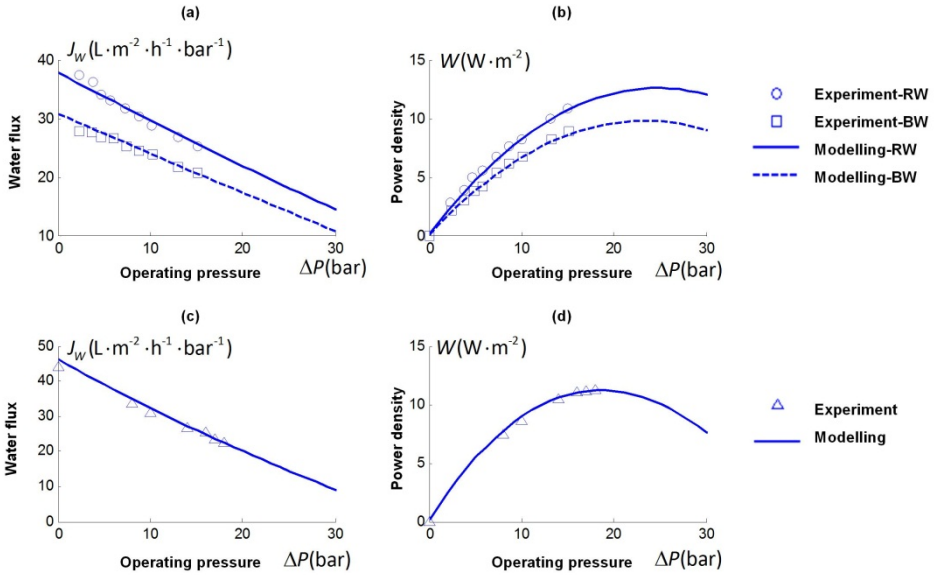

Fig. 3 Validation of the water flux and power density modeled based on the PRO model used in this study. In (a) and (b), the simulation results of water flux and power density are validated with the experimental results from [73]. And in (c) and (d), the simulation results of water flux and power density are validated with the experimental results from [74].

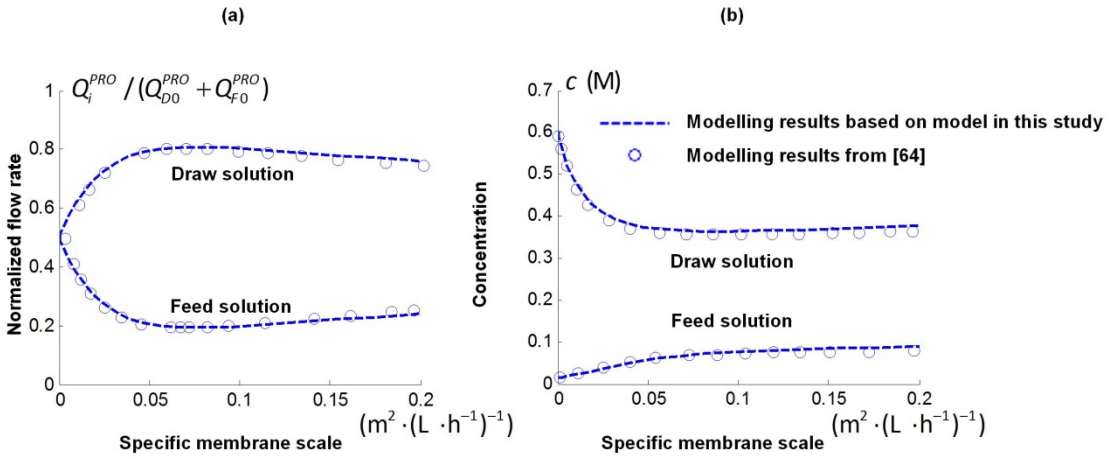

Fig. 4 Comparison between the results based on the scale-up PRO model in this study and the results from [64]. The changing flow rate and concentration of the draw and feed along the flow channel in a scale-up PRO are shown in (a) and (b), respectively. The flow rate is represented by the normalized flow rate which is the flow rate at a given position divided by the total initial flow rate. The subscript i denotes the draw or the feed solution.

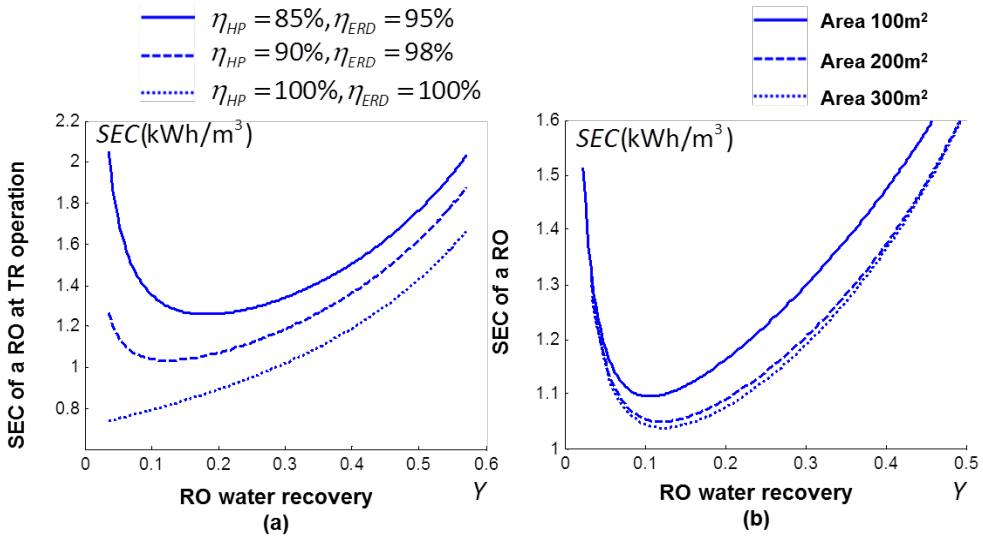

Fig. 5. SEC profile of the RO plant. The SEC profiles of the RO operated at the TR condition are presented in (a). The SEC profiles of the RO plant with different membrane area usage are shown in (b).

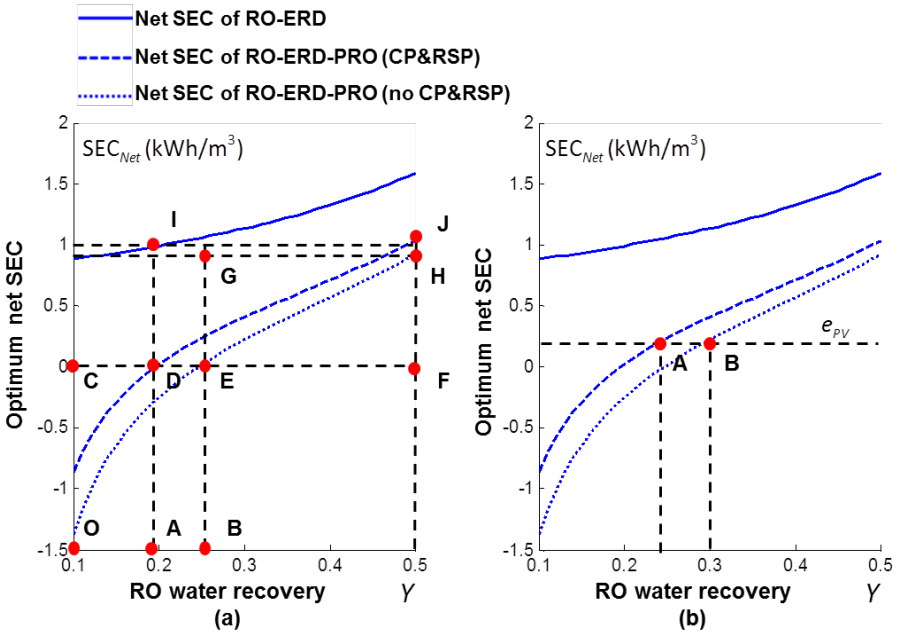

Fig. 6. SEC profiles of RO desalination with osmotic energy recovery by PRO.

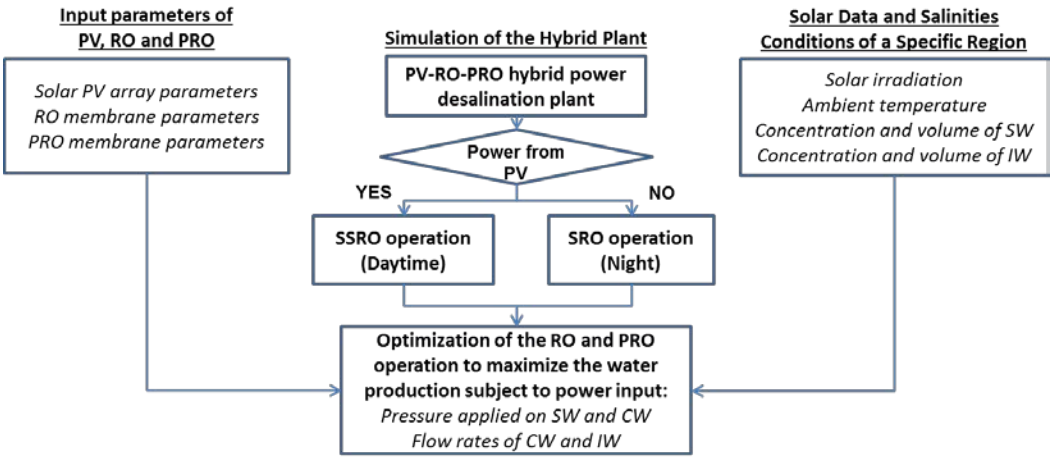

Fig. 7. Illustration of the simulation framework.

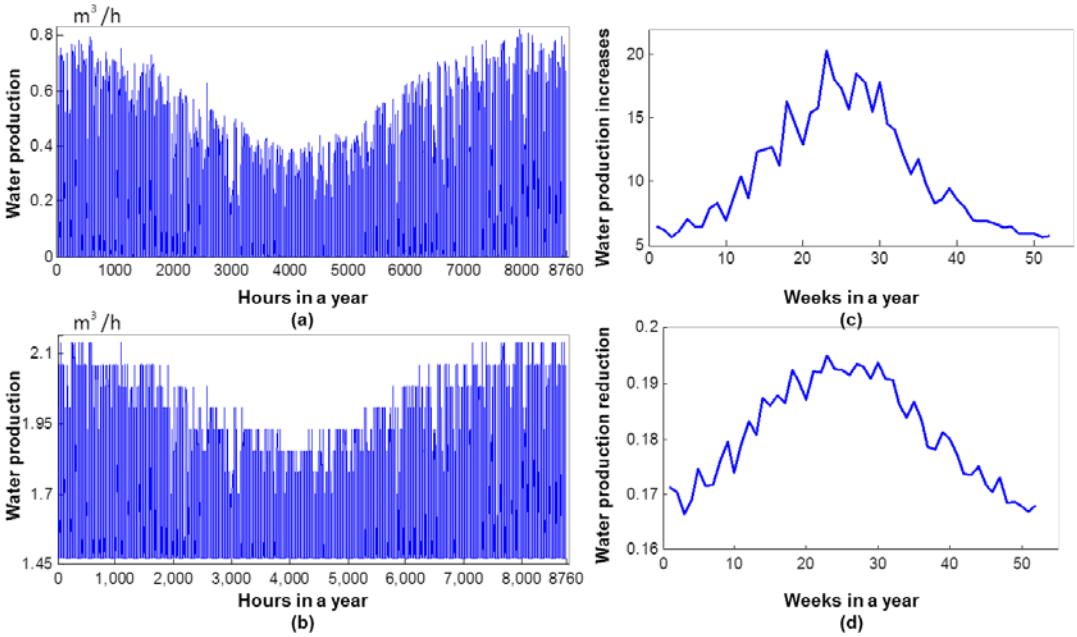

Fig. 8. The stand-alone RO desalination plant. In (a), the hourly water production of the stand-alone PVRO desalination plant are presented. In (b), the hourly water production of the stand-alone PVROPRO desalination plant is shown. The water production increase due to the osmotic energy generation is presented in (c), and the water production reduction due to the CP and RSP effects in PRO plant are presented in (d).

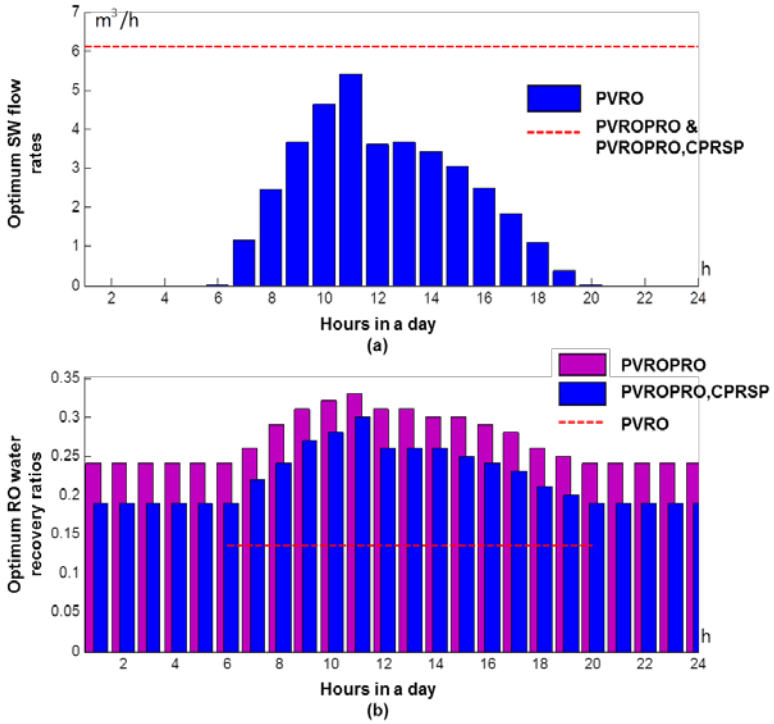

Fig. 9. The optimum operations of the RO plant. In (a), the optimum flow rates of the SW are presented. In (b), the optimum RO water recovery ratios are shown.

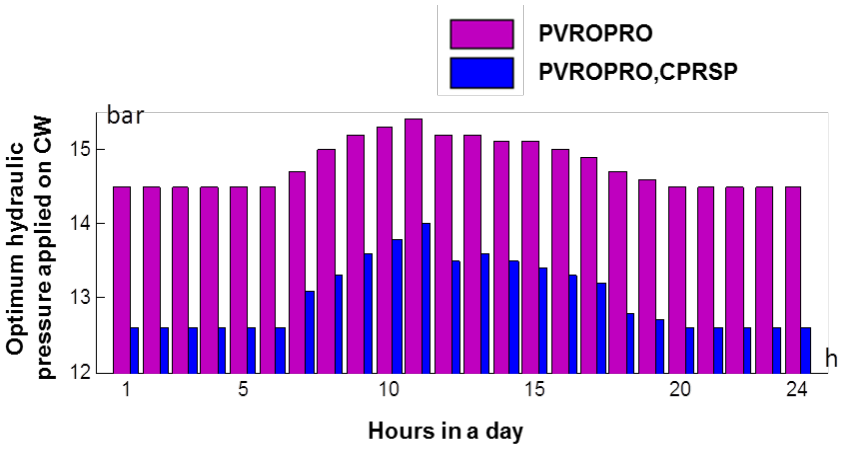

Fig. 10. Optimum hydraulic pressure applied on the CW in the PRO plant.

TABLE 1

Selected membranes and salinities for validation of the water flux equation.

Ref. number	Concentration of the draw solution M	Concentration of the feed solution mM	Membrane water permeability coefficient $L \cdot m^{-2} \cdot h^{-1} \cdot bar^{-1}$	Membrane salt permeability coefficient $L \cdot m^{-2} \cdot h^{-1}$	Membrane structural parameter μm
[73]	1.06	0.9	1.23 ± 0.15	0.28 ± 0.07	149 ± 17
		80			
[74]	1	0	2.5 ± 0.2	0.9	450

TABLE 2
The technical data of solar array Bosch M2453BB

Short-circuit current [A], I_{SC}	8.7	Nominal output [W], P_{mpp}	245
Open-circuit voltage [V], V_{OC}	37.7	Voltage/temperature coefficient [V/K], K_V	-0.1206
Nominal current [A], I_{mpp}	8.2	Current/temperature coefficient [A/K], K_I	0.0028
Nominal voltage [V], V_{mpp}	30.1	Number of series cell, N_S	60